# A dynamic front propagation model for large-eddy simulation of turbulent premixed combustion

**By E. Knudsen, M. Herrmann AND H. Pitsch**

## 1. Motivation and objectives

Turbulent premixed flames are particularly difficult to describe in the context of Large-Eddy Simulation (LES). Most industrially relevant premixed flames exist in either the corrugated flamelets regime or the thin reactions zones regime (Pitsch & Duchamp De Lageneste 2002). The width of the inner reaction zone of a flame in these regimes is comparable to, if not smaller than, the Kolmogorov length scale that describes the size of the smallest turbulent eddies in the flow. Flame preheat zones, which are typically much broader than reaction zones, may also, in the corrugated flamelets regime, exist on sub-Kolmogorov length scales. In LES, by definition, the smallest length scales of a flow are filtered out. As a result, in industrially relevant regimes the transitions that occur between unburned and burned states occur on subfilter scales.

The use of an explicit filtering procedure that could numerically resolve length scales on the order of LES filter widths would permit the simulation of these sharp unburned-to-burned transitions. Most LES codes, however, use implicit filtering. In implicit filtering, filter widths are assumed to correspond to the size of mesh cells. As such, wavenumbers on the order of the filter cutoff are sure to be under-resolved. In some particular cases, turbulence may spread and wrinkle a flame front to the extent that the filtered flame structure is resolvable using implicit filtering. Unfortunately, such a condition can be neither guaranteed nor enforced.

Premixed combustion models for implicitly filtered LES that use standalone progress variable or finite rate chemistry approaches will thus, it seems, always fail. These models are only as accurate as the schemes they use to evaluate gradients. But no scheme is capable of resolving the sharp subgrid transitions that occur in premixed implicit LES near flame fronts. LES models that attempt to resolve flame structure are therefore especially prone to numerical errors in the most critical regions of the flowfield.

This problem has been addressed through the development of application-specific techniques for premixed combustion. Each of the proposed techniques shifts difficulty away from the issue of resolution and toward the issue of modeling (Colin *et al.* 2000; Moureau *et al.* 2006; Pitsch 2005). To ensure success, these techniques must either implicitly or explicitly accomplish two separate tasks. First, they must accurately track the position of filtered flame fronts. Second, given a front position, they must provide an appropriate density field to a flow solver. In most cases, appropriate means resolvable. It does no good to have an accurate representation of a flame front if an unresolved density jump is repeatedly fed into a continuity equation.

For example, the dynamically thickened flame model (Legier *et al.* 2000) uses finite rate chemistry, but additionally broadens local reaction zones so that they can be resolved on LES grids. This broadening is achieved by increasing molecular diffusivities and, in a proportionate manner so as to keep the laminar flame speed constant, spreading out the influence of reaction source terms. The task of providing a resolved density field to

a flow solver is therefore explicitly accomplished by the model. This model suffers from one significant drawback, however, in that the widened flame severely attenuates local turbulence and prevents small eddies from influencing the front. This effectively decreases the velocity at which the front propagates and creates the need for a compensating model. The so-called "efficiency function" that is used acts to ensure that the flame will propagate at appropriately large speeds in the presence of turbulence. This efficiency function may therefore be viewed as the empirical introduction of a model describing the turbulent burning velocity.

Level set approaches such as the $\mathcal{G}$-equation, on the other hand, attempt to explicitly track flame fronts (Pitsch 2005). In these methods, a front is defined as an isocontour of a field variable. This variable is described at the relevant isocontour by a governing equation in which the front propagation velocity directly appears. Away from this isocontour, smooth gradients are prescribed for the field variable to ensure that it is well resolved. As in the thickened flame approach, the influence of subfilter turbulence on the propagation velocity must be modeled. In contrast to the thickened flame approach, however, resolved small-scale eddies are not necessarily damped out and thus do not necessarily need to be modeled. Additionally, and in further contrast, level set methods address the task of returning a density field to a flow solver using flamelet assumptions. Flamelet profiles are typically selected using local flow information and then mapped onto the flame front. In certain level set implementations such as those that use ghost fluids (Moureau *et al.* 2006), it is possible to prescribe subgrid density jumps. In more standard implementations, it will sometimes be necessary to borrow from the thickened flame model and artificially spread the density jump. In such a case the issue of turbulence attenuation is again encountered, but in level set methods dealing with this issue is relatively simple. The parameter used to describe turbulence intensity in the burning velocity model could simply be adjusted.

In summary, it is difficult to describe premixed combustion in the context of LES because premixed flame structures often exist entirely within single grid cells. Widely used approaches to premixed LES such as the thickened flame model and the $\mathcal{G}$-equation address this problem by treating these structures as coherent and then propagating them using a modeled turbulent burning velocity. The turbulent burning velocity is therefore one of the most significant modeling inputs in LES of premixed turbulent combustion. Traditional burning velocity models rely on a series of coefficients that have been tuned by analyzing both experimental and direct numerical simulation (DNS) data (Peters 2000; Abdel-Gayed & Bradley 1981). These coefficient-based approaches have been successfully applied in the context of RANS, where level set methods offer an alternative to the problem of reaction rate closure (Peters 2000; Herrmann 2000). In LES, however, where instantaneous flame realizations are available, it may be possible to eliminate the use of constant coefficients by employing dynamic procedures that determine coefficients automatically.

Im *et al.*, for example, proposed a dynamic level set propagation model in which a level set field variable is treated much like a scalar (Im *et al.* 1997). Subfilter contributions to front propagation are determined by evaluating a burning velocity at two different filter levels and comparing the results to differences in the magnitude of the gradient of the level set field variable at those same two levels. Im *et al.* claim that this approach can be physically interpreted as enforcing flame consumption conservation. They base this claim on work by Kerstein *et al.* demonstrating that a volume average of the magnitude of the gradient of the level set field variable is equivalent to a measure of the total front

area within that volume (Kerstein *et al.* 1988). In Kerstein *et al.*'s work, each isocontour of the level set field variable is treated as an equally valid representation of the flame front. Under this assumption, volume averaging is equivalent to averaging over multiple front realizations.

But more recent work (Peters 2000; Oberlack *et al.* 2001; Pitsch 2005) has stressed that level set governing equations are only valid at the field variable isocontour that they describe, and that traditional averaging procedures therefore cannot be used. Specifically, because the value of a level set field variable can be arbitrarily defined away from the relevant isoconotour, volume averaging procedures can produce arbitrary results. In the present paper, then, a dynamic burning velocity model is proposed that only considers information directly from the 2-D front of interest. This model requires the use of a volumetric surface filter that is developed and presented in Section 2. In Section 3, the new filtering technique is applied to develop the dynamic model. Section 4 presents an evaluation of the model in the context of DNS. Brief conclusions are offered in Section 5.

## 2. Spatial filtering of a surface

Level set equations can be derived by setting the substantial derivative of a generic field variable equal to zero at a surface of interest. The resulting expression describes how the field variable isocontour associated with that surface evolves. In premixed LES, the derivation of an equation governing flame front behavior can be approached in a different way. A flame front can generally be defined as an isocontour of a generic progress variable $c$. This variable might represent, for example, a non-dimensionalized temperature. The equation governing the behavior of such a variable is

$$\frac{\partial c}{\partial t} + u_j \frac{\partial c}{\partial x_j} = \frac{1}{\rho} \frac{\partial}{\partial x_j} \left( \rho D \frac{\partial c}{\partial x_j} \right) + \frac{1}{\rho} \dot{\omega}_R, \tag{2.1}$$

where $u_j$ is the local flow velocity in the $j$th direction, $\rho$ is the fluid density, $D$ is the diffusivity of the variable $c$, and where $\dot{\omega}_R$ is a source term that describes the effects of chemical reactions. To derive an equation describing the flame front associated with a particular $c$ isosurface, information from Eq. (2.1) needs to be extracted directly from this isosurface, here arbitrarily defined as $c = c_0$. This extraction operation can be performed by multiplying Eq. (2.1) with a delta function, $\delta(c - c_0)$,

$$\delta(c - c_0) \left[ \frac{\partial c}{\partial t} + u_j \frac{\partial c}{\partial x_j} \right] = \delta(c - c_0) \left[ \frac{1}{\rho} \frac{\partial}{\partial x_j} \left( \rho D \frac{\partial c}{\partial x_j} \right) + \frac{1}{\rho} \dot{\omega}_R \right]. \tag{2.2}$$

This delta function does not necessarily need to be an infinitesimally thin Dirac delta. Rather, here $\delta$ will be defined as a normalized Gaussian of finite width. As long as this width is an order of magnitude smaller than the length scale associated with the inner reaction zone of a flame, multiplication with $\delta(c - c_0)$ will effectively give a null result everywhere except at the flame front. This finite width definition of $\delta$ is convenient because it eliminates the problem of dealing with the special mathematical properties of the Dirac delta.

Just as Dirac delta functions may equivalently be written as derivatives of heaviside functions, Gaussians may equivalently be written as derivatives of error functions. Since the $\delta$ function that appears in Eq. (2.2) only depends on $c$, the chain rule may be used to rewrite the left-hand side of Eq. (2.2). Remembering that what here will be referred to as the heaviside function $H$ represents an error function of finite width, this procedure

gives

$$\delta\left(c-c_0\right)\left[\frac{\partial c}{\partial t}+u_j\frac{\partial c}{\partial x_j}\right]=\frac{\partial\left[H\left(c-c_0\right)\right]}{\partial t}+u_j\frac{\partial\left[H\left(c-c_0\right)\right]}{\partial x_j}. \tag{2.3}$$

To move the heaviside function on the right-hand side into the relevant derivatives, the gradient of the progress variable must first be written in terms of the front normal direction at $c_0$, which here will be denoted $n_j$.

$$\frac{\partial c}{\partial x_j}=\frac{\nabla c}{|\nabla c|}\left|\nabla c\right|=n_j\left|\nabla c\right| \tag{2.4}$$

Use of the product rule on the diffusive term then gives

$$\frac{\partial}{\partial x_j}\left(\rho D\frac{\partial c}{\partial x_j}\right)=\rho D\frac{\partial n_j}{\partial x_j}\left|\nabla c\right|+n_j\frac{\partial}{\partial x_j}\left(\rho D\left|\nabla c\right|\right). \tag{2.5}$$

Finally, the delta function acts on $|\nabla c|$ as

$$\delta\left(c-c_0\right)\left|\nabla c\right|=\left|\delta\left(c-c_0\right)\nabla c\right|=\left|\nabla\left[H\left(c-c_0\right)\right]\right|. \tag{2.6}$$

Combining all of these elements, the right-hand side of Eq. (2.2) can now be written

$$\delta\left(c-c_0\right)\left[\frac{1}{\rho}\frac{\partial}{\partial x_j}\left(\rho D\frac{\partial c}{\partial x_j}\right)+\frac{1}{\rho}\dot{\omega}_R\right] \quad = \tag{2.7}$$

$$D\kappa|\nabla\left[H\left(c-c_0\right)\right]|+\delta\left(c-c_0\right)\frac{1}{\rho}\left[n_j\frac{\partial}{\partial x_j}\left(\rho D\left|\nabla c\right|\right)+\dot{\omega}_R\right], \tag{2.8}$$

where $\kappa$ is the divergence of the normal vector, or the curvature. The whole equation then becomes

$$\frac{\partial\left[H\left(c-c_0\right)\right]}{\partial t}+u_j\frac{\partial\left[H\left(c-c_0\right)\right]}{\partial x_j} \quad = \tag{2.9}$$

$$D\kappa|\nabla\left[H\left(c-c_0\right)\right]|+\delta\left(c-c_0\right)\frac{1}{\rho}\left[n_j\frac{\partial}{\partial x_j}\left(\rho D\left|\nabla c\right|\right)+\dot{\omega}_R\right]. \tag{2.10}$$

This equation governs the behavior of a heaviside function located at the flame front, and in this form strongly resembles a level set equation. It differs from a level set equation, however, in that the heaviside function is meaningfully defined at all locations in the field away from the front.

A new variable can now be introduced. The variable $G$ will be defined as

$$G=H\left(c-c_0\right), \tag{2.11}$$

where the $G$ field away from $c=c_0$ is not arbitrary but rather obeys the rules of a heaviside function. A universally valid substitution in Eq. (2.10) gives

$$\frac{\partial G}{\partial t}+u_j\frac{\partial G}{\partial x_j}=D\kappa|\nabla G|+\frac{\rho_u}{\rho}s_{L,u}|\nabla G|, \tag{2.12}$$

where

$$\frac{\rho_u}{\rho}s_{L,u}=\frac{\rho_u}{\rho}\frac{1}{\left|\nabla c\right|\rho_u}\left[n_j\frac{\partial}{\partial x_j}\left(\rho D\left|\nabla c\right|\right)+\dot{\omega}_R\right]. \tag{2.13}$$

Here, the quantity $s_L$ describes the laminar burning velocity of the flame, which is a function of the diffusion and source terms in the progress variable equation, as expected. The quantity $\rho_u$ describes the density of the unburned fluid, and is introduced to ensure

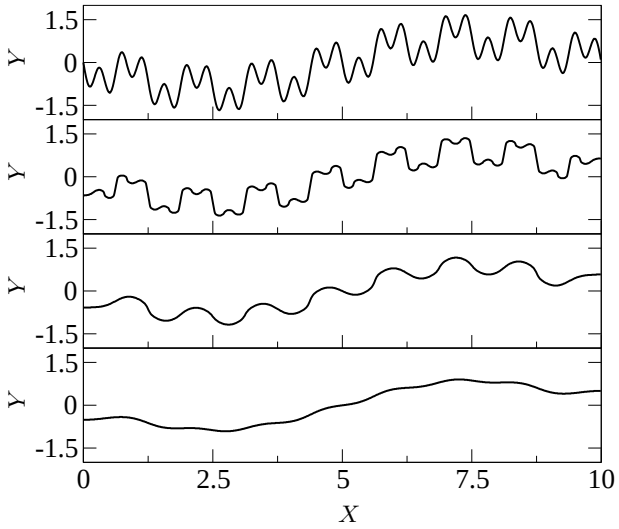


FIGURE 1. Application of Eq. (2.14) to the surface $G = 0$ defined by the field variable $G(X,Y) = 1.8\sin\left(\frac{2\pi X}{10}\right) + \sin\left(\frac{16\pi X}{10}\right) + \sin\left(\frac{48\pi X}{10}\right) + 2Y$. The uppermost plot shows the exact level set. The three lower plots show the level set after sequential filterings. Here, $\mathcal{F}(r)$ is a box filter.

that laminar burning velocities computed in unburned reference frames, $s_{L,u}$, may be used within the equation.

Unlike level set variables, $G$ can be volumetrically filtered because there is nothing arbitrary about its definition. Defining $\mathcal{F}(\mathbf{r})$ to be some appropriately normalized filter kernel and then applying it to the $G$ field gives

$$\overline{G}(\mathbf{x},t) = \int_{|\mathbf{r}|\leq\Delta} \mathcal{F}(\mathbf{r})\, G(\mathbf{x}-\mathbf{r},t)\, d\mathbf{r} = \int_{|\mathbf{r}|\leq\Delta} \mathcal{F}(\mathbf{r})\, H(c(\mathbf{x}-\mathbf{r},t)-c_0)\, d\mathbf{r}, \qquad (2.14)$$

where $\Delta$ is some characteristic filter width. This filtering procedure is consistent with LES in the sense that the same filter kernel $\mathcal{F}(\mathbf{r})$ that is used to filter the Navier-Stokes equations can be used for surface filtering, even when Favre density weighting is considered. It will be assumed here that the filter kernel $\mathcal{F}(\mathbf{r})$ does not change from point to point in physical space $\mathbf{x}$.

Figure 1 demonstrates how the filtering operation proposed in Eq. (2.14) affects a 2-D front consisting of a variety of wavenumbers. As shown, it first removes the highest wavenumbers, as is desirable in LES. After multiple filter passes, only the lowest wavenumber mode remains.

To summarize, Eq. (2.12) governs the evolution of a heaviside function that describes the flame front. Because this equation is valid everywhere, it can be volumetrically filtered and easily manipulated. It is not numerically tractable, however, since it describes sharp jumps. A level set equation will therefore have to be introduced if simulations are to be performed.

A level set field variable $\mathcal{G}$ associated with an unfiltered flame front can be defined as

$$\mathcal{G} = \mathcal{G}_0 \quad \forall \quad c = c_0 \quad (\ \textit{equivalently},\ \forall\ \ G = G_0\ ) \qquad (2.15)$$

$$|\nabla\mathcal{G}| = 1 \quad \forall \quad c \neq c_0 \quad (\ \textit{equivalently},\ \forall\ \ G \neq G_0\ )\,, \qquad (2.16)$$

where the definition away from the $c_0$ surface is arbitrary. Equation (2.15) guarantees

that the $c_0$ and $\mathcal{G}_0$ surfaces evolve in tandem. A governing equation for $\mathcal{G}$ can be developed by following the level set derivation procedure mentioned at the beginning of this section. Taking the substantial derivative of Eq. (2.15) yields

$$\left.\frac{\mathbf{D}\mathcal{G}}{\mathbf{D}t}\right|_{\mathcal{G}=\mathcal{G}_0} = \left.\frac{\partial\mathcal{G}}{\partial t}\right|_{\mathcal{G}=\mathcal{G}_0} + \mathrm{v}_{j,\mathcal{G}_0}\left.\frac{\partial\mathcal{G}}{\partial x_j}\right|_{\mathcal{G}=\mathcal{G}_0} = 0, \tag{2.17}$$

where $\mathrm{v}_{j,\mathcal{G}_0}$ describes the combined influence of propagation and convection on the $\mathcal{G}_0$ front. $\mathrm{v}_{j,\mathcal{G}_0}$ is not arbitrary but rather is implicitly defined by Eq. (2.15). Specifically, it is what forces the $\mathcal{G}_0$ surface to evolve in tandem with $c_0$. Since the convection and propagation speeds of $c$ are explicitly available from Eq. (2.10) (or, equivalently, from Eq. (2.12)), however, $\mathrm{v}_{j,\mathcal{G}_0}$ may simply be written

$$\mathrm{v}_{j,\mathcal{G}_0} = u_j + n_j\left(D\kappa + s_L\right) \tag{2.18}$$

where again

$$s_L = \frac{\rho_u}{\rho}s_{L,u} = \frac{\rho_u}{\rho\left|\nabla c\right|}\frac{1}{\rho_u}\left[n_j\frac{\partial}{\partial x_j}\left(\rho D\left|\nabla c\right|\right) + \dot{\omega}_R\right]. \tag{2.19}$$

After substituting for $\mathrm{v}_{j,\mathcal{G}_0}$ at the front, the level set equation becomes

$$\frac{\partial\mathcal{G}}{\partial t} + u_j\frac{\partial\mathcal{G}}{\partial x_j} = D\kappa|\nabla\mathcal{G}| + \frac{\rho_u}{\rho}s_{L,u}|\nabla\mathcal{G}| \quad \forall \quad \mathcal{G}=\mathcal{G}_0. \tag{2.20}$$

At all locations away from the $\mathcal{G}_0$ surface, $\mathcal{G}$ obeys no governing equation because it is arbitrarily defined.

Eq. (2.18) provides a critical link between Eq. (2.12) and Eq. (2.20). When $G$ is filtered this link changes, but it does so in a completely consistent way. The filtered variable $\overline{G}$ and its governing equation can be used to derive a level set equation at the filter level $\overline{u}_j$. For example, consider an unfiltered flame front described by a heaviside function such as is done in Eq. (2.11). Eq. (2.12) governs the behavior of this heaviside function. If a LES of the flame front is to be performed using a filter kernel $\mathcal{F}$, the corresponding filtered front can be found using Eq. (2.14). Furthermore, filtering Eq. (2.12) with the operator in Eq. (2.14) will yield an appropriate filtered governing equation. Since the $\overline{G}$ equation is not numerically tractable, however, a level set equation describing the same surface must be developed. The corresponding level set field variable $\overline{\mathcal{G}}$ would be defined by

$$\overline{\mathcal{G}} = \mathcal{G}_0 \quad \forall \quad \overline{G} = G_0 \tag{2.21}$$

$$\left|\nabla\overline{\mathcal{G}}\right| = 1 \quad \forall \quad \overline{G} \neq G_0. \tag{2.22}$$

The governing level set equation at the front would make use of some filtered velocity $\overline{\mathrm{v}}_{j,\overline{\mathcal{G}}_0}$. Unlike the unfiltered case, however, it is not easy to explicitly write down what this velocity should be. The unclosed terms that appear when a filter is applied to Eq. (2.12) must be modeled. They can then be used in the level set equation associated with the relevant filter level.

The results of filtering Eq. (2.12) will now be examined, and a dynamic model describing subfilter effects will be developed. The results of this model will be applicable at $\overline{\mathcal{G}} = \mathcal{G}_0$, thus closing the problems of both filtering and numerical tractability.

## 3. Dynamic propagation model

With an appropriate surface filtering procedure defined, it is possible to derive a dynamic identity that describes the speed at which a turbulent front propagates. This

identity will be derived using Eq. (2.12). In many respects, it resembles Germano's identity. A particular form of the latter appears when the Navier-Stokes equations are written at two different filter levels, here denoted with respect to the velocity $u_j$ by $\overline{u}_j$ and $\overline{\overline{u}}_j$.

$$\frac{\partial \overline{u}_i}{\partial t} + \frac{\partial}{\partial x_j}\left(\overline{u}_i \overline{u}_j\right) + \frac{\partial}{\partial x_j}\left(\overline{u_i u_j} - \overline{u}_i \overline{u}_j\right) = \overline{RHS} \tag{3.1}$$

$$\frac{\partial \overline{\overline{u}}_i}{\partial t} + \frac{\partial}{\partial x_j}\left(\overline{\overline{u}}_i \overline{\overline{u}}_j\right) + \frac{\partial}{\partial x_j}\left(\widehat{\overline{u_i u_j}} - \overline{\overline{u}}_i \overline{\overline{u}}_j\right) = \widehat{\overline{RHS}}, \tag{3.2}$$

where $RHS$ describes the pressure, diffusive, and body force terms, and where a constant density assumption has been made for simplicity. Applying the filter $\overline{\overline{u}}_j$ to Eq. (3.1) and then subtracting Eq. (3.2) gives

$$\frac{\partial}{\partial x_j}\widehat{\left(\overline{u}_i \overline{u}_j\right)} - \frac{\partial}{\partial x_j}\left(\overline{\overline{u}}_i \overline{\overline{u}}_j\right) = \frac{\partial}{\partial x_j}\left(\widehat{\overline{u_i u_j}} - \overline{\overline{u}}_i \overline{\overline{u}}_j\right) - \frac{\partial}{\partial x_j}\widehat{\left(\overline{u_i u_j} - \overline{u}_i \overline{u}_j\right)}, \tag{3.3}$$

where the fact that the right-hand sides of the Navier-Stokes equations commute with filters has been used. It has also been assumed that

$$\widehat{\left(\overline{u}_i\right)} = \overline{u}_i, \tag{3.4}$$

which is not necessarily true for an arbitrary filter $\mathcal{F}$. If all subfilter quantities are known, then Eq. (3.3), which is the spatial gradient of Germano's identity, will trivially reduce to $0 = 0$. When subfilter quantities are modeled, however, this equation does not identically hold. But employing a model that enforces this equation ensures that even when subfilter errors are made, the evolution of a doubly filtered velocity field matches the filtered evolution of a singly filtered velocity field. This condition should always be true in consistent LES procedures.

A similar analysis may be performed on a surface evolution equation. When a single filter is applied, Eq. (2.12) becomes

$$\frac{\partial \overline{G}}{\partial t} + \overline{u}_j \frac{\partial \overline{G}}{\partial x_j} + \overline{u'_j \frac{\partial G}{\partial x_j}} = D\overline{\kappa}\overline{|\nabla G|} + D\overline{\kappa' |\nabla G|} + \frac{\rho_u}{\overline{\rho}}\overline{s}_{sgs}\left|\nabla \overline{G}\right|, \tag{3.5}$$

where $\frac{\rho_u}{\overline{\rho}}\overline{s}_{sgs}\left|\nabla \overline{G}\right|$ is the turbulent front propagation model corresponding to the filter size,

$$\frac{\rho_u}{\overline{\rho}}\overline{s}_{sgs}\left|\nabla \overline{G}\right| = \overline{\frac{\rho_u}{\rho} s_{L,u} |\nabla G|}, \tag{3.6}$$

and where primed quantities are defined as

$$\phi'(\mathbf{x}, \mathbf{r}, t) = \phi(\mathbf{x} - \mathbf{r}, t) - \overline{\phi}(\mathbf{x}, t). \tag{3.7}$$

When a second, broader filter is used, the equation becomes

$$\frac{\partial \overline{\overline{G}}}{\partial t} + \overline{\overline{u}}_j \frac{\partial \overline{\overline{G}}}{\partial x_j} + \widehat{\overline{u''_j \frac{\partial G}{\partial x_j}}} = D\overline{\overline{\kappa}}\widehat{\overline{|\nabla G|}} + D\widehat{\overline{\kappa'' |\nabla G|}} + \frac{\rho_u}{\overline{\rho}}\overline{s}_{sgs}\left|\nabla \overline{\overline{G}}\right|, \tag{3.8}$$

where the double prime denotes

$$\phi''(\mathbf{x}, \mathbf{r}, t) = \phi(\mathbf{x} - \mathbf{r}, t) - \overline{\phi}(\mathbf{x}, t). \tag{3.9}$$

Like $\overline{u}_j$, $\overline{\kappa}$ is defined everywhere in the vicinity of the front, since $\kappa = \nabla \cdot \left(\frac{\nabla c}{|\nabla c|}\right)$. When

multiplied with $G$, however, these filtered quantities become irrelevant at all locations away from the flame front.

It is interesting to note what happens when Favre velocity filtering is used. Then, filtered velocities $\overline{u}_j$ are defined as

$$\overline{u}_j(\mathbf{x},t) = \frac{1}{\overline{\rho}(\mathbf{x},t)} \int_{|\mathbf{r}|\leq\Delta} \mathcal{F}(\mathbf{r})\,\rho(\mathbf{x}-\mathbf{r},t)\,u_j(\mathbf{x}-\mathbf{r},t)\,d\mathbf{r} \tag{3.10}$$

and fluctuating velocities as

$$u'_j(\mathbf{x},\mathbf{r},t) = u_j(\mathbf{x}-\mathbf{r},t) - \frac{1}{\overline{\rho}(\mathbf{x},t)} \int_{|\mathbf{r}|\leq\Delta} \mathcal{F}(\mathbf{r})\,\rho(\mathbf{x}-\mathbf{r},t)\,u_j(\mathbf{x}-\mathbf{r},t)\,d\mathbf{r}. \tag{3.11}$$

Again, when these velocity fluctuations are multiplied with spatial derivatives of $G = H(c-c_0)$ in Eq. (3.5), information is retained only directly at the front. As such, the $\overline{\rho}(\mathbf{x},t)$ term that appears in Eq. (3.11) takes on the value of the front conditioned density, $\overline{\rho}(\mathbf{x},t) = \overline{\rho}(c_0)$, when it appears in the level set equation. In this sense, all fluctuating velocities in the equation are conditioned on the density at the front.

A simplification unique to surfaces can now be introduced. Intuition suggests that all filtered combinations of fluctuating velocities and $G$ are approximately zero,

$$\overline{u'_j \frac{\partial G}{\partial x_j}} \approx 0, \qquad \widehat{\overline{u''_j \frac{\partial G}{\partial x_j}}} \approx 0. \tag{3.12}$$

Specifically, these terms describe how high wavenumber velocity components move the filtered front. They tend to wrinkle the instantaneous front, but they act only along a 2-D surface within the filter volume. When these terms are filtered, therefore, they will on average have no effect on the mean front position. Some of the subfilter velocity fluctuations will tend to move the subfilter front location forward, and some will tend to move the front location backward. But because these fluctuations are all deviations from the local filtered velocity, when integrated along the front over the filter volume, they will all tend to cancel out. For example, if a non-propagating front were released in a flowfield of homogeneous isotropic turbulence, subfilter scale velocity fluctuations would exist. But the mean front position would remain stationary, even though the exact front becomes more and more wrinkled. These terms should therefore be unable to contribute to front propagation.

Filtering Eq. (3.5), subtracting Eq. (3.8), and manipulating produces

$$\overline{\left(\overline{u}_j - \widehat{\overline{u}}_j\right) \frac{\partial \overline{G}}{\partial x_j}} = D\widehat{\overline{\overline{\kappa}|\nabla G|}} - D\widehat{\overline{\kappa}}\widehat{|\nabla G|} + \tag{3.13}$$

$$\widehat{\left(\overline{D}_{G,sgs}\right)} - \widehat{\overline{D}}_{G,sgs} + \frac{\rho_u}{\overline{\rho}} \left( \widehat{\overline{s}_{sgs}\left|\nabla \overline{G}\right|} - \widehat{\overline{s}}_{sgs}\left|\nabla \widehat{\overline{G}}\right| \right), \tag{3.14}$$

where the filtered density at the front is taken to be independent of the filter level. Again, the term on the left-hand side describes the effect of filtered velocity fluctuations and so can be dropped. $D_{G,sgs}$ is the model used to describe subfilter curvature induced front propagation,

$$\overline{D}_{G,sgs} = D\overline{\kappa'|\nabla G|}, \qquad \widehat{\overline{D}}_{G,sgs} = D\widehat{\overline{\kappa''|\nabla G|}}. \tag{3.15}$$

Upon grouping all curvature related terms together into $\mathscr{D}$,

$$\mathscr{D} = D\overline{\kappa}\widehat{|\nabla G|} - D\widehat{\overline{\kappa}|\nabla G|} + \widehat{\left(\overline{D}_{G,sgs}\right)} - \widehat{\overline{D}}_{G,sgs} \tag{3.16}$$

the dynamic identity becomes

$$\frac{\widehat{\overline{\rho}}}{\rho_u}\mathscr{D} = \widehat{\overline{s}_{sgs}\left|\nabla\overline{G}\right|} - \overline{s}_{sgs}\left|\nabla\widehat{\overline{G}}\right|. \tag{3.17}$$

For the purposes of simplification, the remainder of this brief will consider the corrugated flamelets regime only. Diffusive effects in this regime do no significantly influence the burning velocity, resulting in $\mathscr{D} \approx 0$. In this regime, then, the identity reduces to

$$\overline{s}_{sgs}\left|\nabla\widehat{\overline{G}}\right| = \widehat{\overline{s}_{sgs}\left|\nabla\overline{G}\right|}. \tag{3.18}$$

LES turbulent burning velocity models usually depend much more strongly on the filtering level at which they act than on space. $\overline{s}_{sgs}$ may therefore be drawn outside the filter integral, leaving

$$\frac{\widehat{\overline{s}}_{sgs}}{\overline{s}_{sgs}} = \frac{\widehat{\left|\nabla\overline{G}\right|}}{\left|\nabla\widehat{\overline{G}}\right|}. \tag{3.19}$$

Although this equation looks very much like a dynamic identity, the $G$ variable will not be available in computations. Eq. (3.19) can be written in a more useful form by manipulating the filter definition. If for the purposes of demonstration the first filter level is taken to represent a completely resolved field, then

$$\widehat{\left|\nabla\overline{G}\right|} = \widehat{|\nabla G|} = \int_{r\leq 2\Delta} \mathcal{F}_{2\Delta}\left(\mathbf{r}\right)\left|\nabla H\left(c\left(\mathbf{x}-\mathbf{r},t\right)-c_0\right)\right| d\mathbf{r} \tag{3.20}$$

$$= \int_{r\leq 2\Delta} \mathcal{F}_{2\Delta}\left(\mathbf{r}\right)\delta\left(c\left(\mathbf{x}-\mathbf{r},t\right)-c_0\right)\left|\nabla c\left(\mathbf{x}-\mathbf{r},t\right)\right| d\mathbf{r}. \tag{3.21}$$

It will now be assumed that $|\nabla c|$ does not strongly vary along the flame front. In the corrugated flamelets and thin reaction zones regimes this assumption is certain to hold since turbulent eddies do not penetrate the inner reaction zones of such flames. Under this assumption, $|\nabla c|$ may be treated as a constant and brought out of the integral. Additionally, a front area per filter volume may be defined as

$$a_{2\Delta} = \int_{r\leq 2\Delta} \mathcal{F}_{2\Delta}\left(\mathbf{r}\right)\delta\left(c\left(\mathbf{x}-\mathbf{r},t\right)-c_0\right) d\mathbf{r}. \tag{3.22}$$

When $\mathcal{F}$ is a tophat filter, $a_{2\Delta}$ describes the exact unfiltered flame area within the filter domain. When $\mathcal{F}$ is a Gaussian, $a_{2\Delta}$ gives flame surfaces near the center of the filtering domain more weight. Using these assumptions, $\widehat{|\nabla G|}$ may be rewritten

$$\widehat{|\nabla G|} = \left|\nabla c\right|\big|_{c_0} a_{2\Delta}. \tag{3.23}$$

The denominator of the right hand side of Eq. (3.19) may be written

$$\left|\nabla\overline{G}\right| = \left|\nabla c\right|\big|_{c_0}\left|\int_{r\leq 2\Delta} \mathcal{F}_{2\Delta}\left(\mathbf{r}\right)\delta\left(c\left(\mathbf{x}-\mathbf{r},t\right)-c_0\right) n_j\left(\mathbf{x}-\mathbf{r},t\right) d\mathbf{r}\right| \tag{3.24}$$

It can be shown that the expression within the absolute value sign describes the area

density of the *filtered* flame front within the filter volume. This quantity will be defined as $\overline{a}_{2\Delta}$. Finally, since the right-hand side of Eq. (3.19) describes flame area densities within the same filter volume, the actual flame areas may be used in the identity,

$$\frac{\overline{\overline{s}}_{sgs}}{\overline{s}_{sgs}} = \frac{\overline{A}_{front}}{\overline{\overline{A}}_{front}}. \tag{3.25}$$

This form of the identity agrees with Damkohler's hypothesis (Damköhler 1941),

$$\frac{s_T}{s_L} \sim \frac{A_{exact}}{A_{mean}}, \tag{3.26}$$

and enforces the condition that the mass a flame consumes should be independent of filter level.

The remainder of this brief will use a burning velocity model proposed by Peters (Pitsch 2005), (Peters 2000),

$$\frac{s_T - s_L}{u'} = -\gamma \mathrm{Da} + \sqrt{(\gamma \mathrm{Da})^2 + \gamma \alpha \mathrm{Da}}. \tag{3.27}$$

In the limits of large and small Da, respectively, this model reduces to

$$s_T = s_L + u' \frac{\alpha}{2}, \qquad\qquad s_T = s_L \left(1 + (\gamma\alpha)^{\frac{1}{2}} \sqrt{\frac{D_t}{D}}\right), \tag{3.28}$$

which obey the appropriate regime scaling laws. While it is not entirely clear that the placement of the $\alpha$ and $\gamma$ coefficients in Eq. (3.27) is ideal, it is reasonable to suggest that physically, flame mass consumption should appear in both limiting cases. Therefore, Eq. (3.25) will be used as a dynamic identity, Eq. (3.27) will be used to model $s_{sgs}$, and $\alpha$ in Eq. (3.27) will be treated as a dynamic coefficient.

## 4. DNS results

A direct numerical simulation (DNS) of a front propagating in forced homogeneous isotropic turbulence was performed to validate this model. The parameters describing the DNS are shown in Table 1. Turbulence was forced using the linear scheme of Rosales and Meneveau (Rosales & Meneveau 2005), and the simulation was run at a constant density. A uniform cartesian mesh was used, but in the direction of front propagation the domain length was doubled so that front statistics could be gathered for a longer period of time. The level set equation

$$\frac{\partial \mathcal{G}}{\partial t} + u_j \frac{\partial \mathcal{G}}{\partial x_j} = s_L \left|\nabla \mathcal{G}\right| \quad \forall \quad \mathcal{G} = \mathcal{G}_0 \tag{4.1}$$

was solved to describe front evolution. As there are no diffusive terms in this equation, the front effectively propagates with a Damkohler number of infinity, and thus resides in the corrugated flamelets regime. A re-initialization procedure was performed after every three time steps to force the level set field variable away from the front to conform to a distance function. Reinitialization was accomplished by first using an iterative marker method to estimate the distance to the front, and subsequently solving a PDE in psuedo-time to improve the accuracy of this estimate. The third order WENO scheme of Peng *et al.* (Peng *et al.* 1999) was used for the PDE step.

Statistics involving the front itself were computed using information from only one

| Simulation Constants | Turbulence Parameters |
|---|---|
| Mesh Size = 256 x 128 x 128 | $Re_\lambda = 39$ |
| $\Delta x = 1.0 \cdot 10^{-3}\ m$ | $Re_t = 101$ |
| $\nu = 1.87 \cdot 10^{-5}\ m^2 \cdot s^{-1}$ | Integral length scale, $l_t = 7.7 \cdot 10^{-3}\ m$ |
| $\rho = 1.16\ kg \cdot m^{-3}$ | Eddy turnover time, $\tau = 0.20\ s$ |
| Burning velocity, $s_L = 0.06\ m \cdot s^{-1}$ | Komogorov scale, $\eta = 5.0 \cdot 10^{-4}\ m$ |
| Forcing Coefficient, $A = 2.4$ | Largest eddy size, $l = 16.0 \cdot 10^{-3}\ m$ |

TABLE 1. DNS Parameters

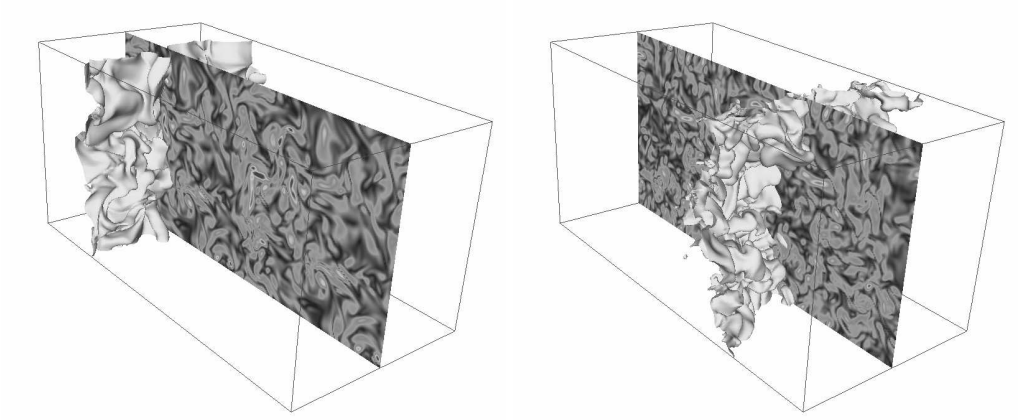

FIGURE 2. Snapshots from a DNS of front propagation. The level set is the wrinkled surface, and the cut plane shows voriticity magnitude. The left image shows an early time in the simulation, while the right image shows the fully developed front.

isocontour of the level set field variable. Neumann boundary conditions were prescribed for the level set at each end of the domain in the propagation direction. The front, however, never comes so near these boundaries that their treatment influences behavior. The front was not allowed to propagate periodically in this direction because the re-initialization procedure would create artificial fronts at the domain boundary. Periodic boundary conditions were prescribed for the level set in the other two directions.

A parallel, structured code that is second order in both time and space was used to compute the flow. Although the code was run using an implicit solver, the CFL number was limited to 0.5 to ensure that all structures were time resolved. Because the linear forcing scheme used here adds energy to the flow at all wavenumbers, the turbulent flowfield was initialized within a $128^3$ cube, and then copied to an adjacent cube. This prevented the generation of wavenumbers smaller than the inverse of the box size. Periodic boundary conditions were used in every direction for the velocity field. Figure 2 shows two instantaneous realizations of the flowfield and front.

Figure 3 shows mean front displacement as a function of time, computed both directly from the DNS and from a variety of models. If no turbulent burning velocity model is used, front displacement is severely under-predicted, as expected. The static turbulent burning velocity model of Eq. (3.27), however, somewhat over-predicts front displacement. This over-prediction primarily develops at early times as the front, which is initially flat, transitions to a wrinkled surface under the influence of turbulence. In

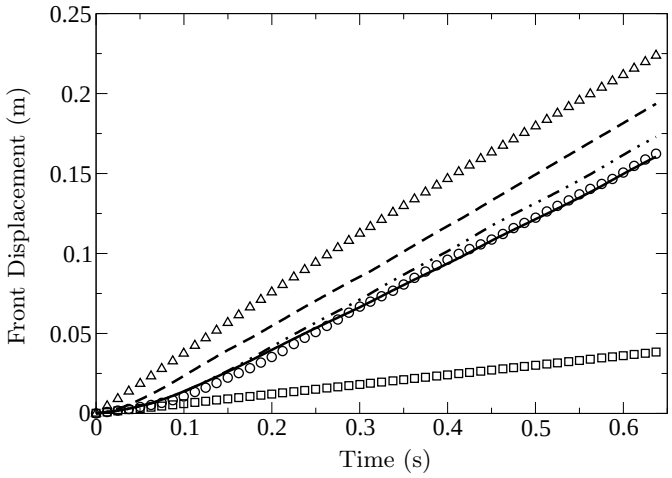


FIGURE 3. Front displacement from initial location as a function of time, using: ○ : Mean front position from DNS; □ : Laminar burning velocity; △ : Static turbulent burning velocity model (Eq. (3.27)); —— : $s_L \frac{A_{unfiltered}}{A_{flat}}$ , with area ratio from DNS; – – : Dynamic model computed using unfiltered and singly filtered fields, – · · – : Dynamic model computed using quadruply filtered and completely filtered fields

contrast, the dynamic model accurately predicts this transition. The solid line, for example, uses unfiltered fields to describe a first filter level, and completely filtered fields to describe a second. Applying Eq. (3.25) in this context consists of multiplying the laminar burning velocity by the area of the fully resolved front and then dividing the result by the width and height of the domain, which represents the area of the completely filtered front. The results are in excellent agreement with the DNS data.

The dynamic model produces results that are somewhat less accurate when filter levels that are very closely spaced are used. For example, when unfiltered and singly filtered fields are used in Eq. (3.25), front displacement is mildly over-predicted. This error does not signify a problem with the modeling approach as much as it highlights the difficulty of describing how velocity fluctuations, $u'$, change with very small changes in filter wavenumber. If the fluctuations are relatively small to begin with, as they are when a singly filtered field is used, all errors made in predicting $u'$ will strongly affect the solution of Eq. (3.25). Similar conclusions were arrived at by Im *et al.* in the context of scalar isosurfaces (Im *et al.* 1997).

Difficulties in predicting filtered velocity fluctuations are alleviated to a certain extent when the test filters selected span a wider range of wavenumbers. The – · · – line in Fig. 3 shows that dynamic model predictions considerably improve when quadruply filtered and completely filtered fields are used as test levels.

Figure 4 shows speeds and area ratios from both the DNS and the models as a function of time. The front propagation speed that the static turbulent burning velocity model predicts varies smoothly in time, because it depends only on averaged velocity fluctuations that are a function of the amount of kinetic energy in the domain. The actual front propagation velocity, however, oscillates at relatively high frequency. The dynamic model, regardless of the filters used, appropriately captures this high frequency behavior, which appears through the surface area of the front. Specifically, even in the dynamic case that uses unfiltered and singly filtered fields, the area ratio of the fronts that is plotted using the right vertical axis qualitatively matches the plot of the DNS front propagation

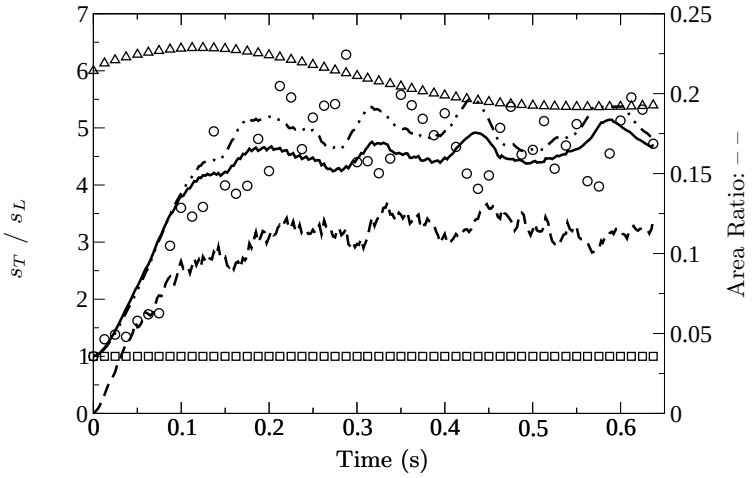


FIGURE 4. Front speed and area ratio as a function of time: ∘ : $s_T$ directly from DNS data; □ : Laminar; △ : Static $s_T$ model (Eq. (3.27)); —— : $\frac{s_T}{s_L} = \frac{A_{unfiltered}}{A_{flat}}$ , with area ratio from DNS; – – : Area ratio of unfiltered and singly filtered fronts (right vertical axis), – · · – : $s_T$ from dynamic model, computed using quadruply filtered and completely filtered fields

speed. The errors in the model are therefore due to the scaling of this area ratio, which again is a function of subfilter velocity fluctuations.

Finally, since the model's sensitivity to $u'$ has been emphasized, it is appropriate to describe how this quantity is computed in the DNS. The most critical requirement for this computation is that there be a match between the filtering procedure used on the front area and the procedure used on the velocity field. At a minimum, this means that the filtering kernel $\mathcal{F}$ that is computationally applied to the front should be the same as that applied to the velocity field. Experience showed, however, that this alone was not enough. Attempts to extract differences in $u'$ from turbulent viscosities computed at two filter levels, or from model turbulence spectra mapped onto the velocity fields, proved insufficient. Rather, the energy of the velocity fields at each filter level had to be computed. A difference in the velocity fluctuations associated with different filters could then be formed,

$$\widehat{\overline{u'}} - \overline{u'} = \sqrt{\frac{2}{3}\overline{k}} - \sqrt{\frac{2}{3}\overline{k}}, \tag{4.2}$$

where $\overline{k}$ is the kinetic energy associated with the velocity field $\overline{u}_j$. Even when an arbitrary means of computing $\overline{u'}$ was used, this technique accurately described how velocity fluctuations varied with the filter used.

## 5. Conclusions

Most computationally tractable methods of simulating turbulent premixed combustion require information regarding the speed of flame front propagation. In this brief, a dynamic model for calculating this speed was presented. First, a consistent flame front filtering approach for LES was developed. This approach is useful because it both works in conjunction with standard LES filtering techniques and because it uses information from just a single 2-D surface. Next, this filtering approach was used to derive a dynamic identity that is compatible with a level set equation. When enforced, this identity en-

sures that evolving a flame front and then filtering the result yields the same answer that evolving a filtered front does. This dynamic identity, in its simplest form, may physically be viewed as an enforcement of flame mass consumption conservation. A DNS was performed to validate the proposed dynamic model. Results showed that the model predicts the speed of a propagating turbulent front with considerably more accuracy than a static burning velocity model.

## 6. Acknowledgements

Support from the United States Department of Defense NDSEG Fellowship Program, and from the United States Air Force Office of Scientific Research (AFOSR), is gratefully acknowledged.

## REFERENCES

Abdel-Gayed R. G., and Bradley D. 1981. A two-eddy theory of premixed turbulent flame propagation. *Philosophical Transactions of the Royal Society of London A* vol. **301**, no. **1457**, 1–25.

Colin O., Ducros F., Veynante D., and Poinsot T. 2000. A thickened flame model for large eddy simulations of turbulent premixed combustion. *Phys. Fluids* **12**, 1843–1862.

Damköhler G. 1941. Der Einfluß der Turbulenz auf die Flammengeschwindigkeit in Gasgemischen. *Z. Elektrochem.* **46**, 601–652, English Translation NASA Tech. Mem. 1112.

Herrmann M. 2000. Numerische simulation vorgemischter und teilweise vorgemischter turbulenter flammen. *Dissertation*, RWTH Aachen.

Im H. G., Lund T. S. and Ferziger J. H. 1997. Large eddy simulation of turbulent front propagation with dynamic subgrid models. *Phys. Fluids* **9**, 3826–3833.

Kerstein A. R., Ashurst W. T. and Williams F. A. 1988. Field equation for interface propagation in an unsteady homogeneous flow field. *Phys. Review A* **37** no. **7**, 2728–2731.

Legier J. P., Poinsot T., and Veynante D. 2000. Dynamically thickened flame LES model for premixed and non-premixed turbulent combustion. *Proc. 2000 CTR Summer Program, Stanford University.*

Moureau V., Minot P., Berat C., and Pitsch H. 2006. A ghost-fluid method for large-eddy simulation of premixed combustion in complex geometries. *J. Computational Physics, in Press.*

Oberlack M., Wenzel H. and Peters N. 2001. On symmetries and averaging of the G-equation for premixed combustion. *Combust. Theory Modelling*, **5**, 363–383.

Peng D., Merriman B., Osher S., Zhao H., and Kang M. 1999. A PDE-Based fast local level set method. *J. Computational Physics*, **155**, 410–438.

Peters N. 2000. Turbulent combustion. Cambridge University Press.

Pitsch H. and Duchamp De Lageneste L. 2002. Large-eddy simulation of premixed turbulent combustion using a level set approach. *Proc. Combustion Institute* **29**, 2001–2008.

Pitsch H. 2005. A consistent level set formulation for large-eddy simulation of premixed turbulent combustion. *Combust. Flame*, **143**, 587–598.

Rosales C. and Meneveau C. 2005. Linear forcing in numerical simulations of isotropic turbulence: physical space implementations and convergence properties. *Phys. Fluids* **17**, 1–8.